Supplementary Information for

Cu-Doped Mesoporous TiO_2 Interlayer for Highly Efficient and Stable Hybrid Perovskite Solar Cells

Jiyoon Kim‡, Kwangchan An‡, Nasrin Siraj Lopa, Santosh V. Mohite, Yeonho Kim, and Tae Woong Kim**

Department of Energy Materials Science & Engineering, College of Science and Technology, Konkuk University, Chungcheongbuk-do 27478, Republic of Korea.

‡J. Kim and K. An contributed equally to this work.

* Corresponding authors: yeonho@kku.ac.kr, taewoongkim@kku.ac.kr

Synthesis of FAI and $FAPbI_3$

Formamidinium iodide (FAI) was synthesized by reacting 25 g of formamidinium acetate (FAAc) with 50 mL of hydroiodic acid (HI, 57 wt% in H_2O) under stirring at 0 °C for 2 h. The resulting FAI precipitate was isolated by removing the solvent using a rotary evaporator at 80 °C for 1 h. The crude product was further purified via recrystallization in ethanol and diethyl ether, collected by filtration, and dried in a vacuum oven at 60 °C for 24 h.

Formamidinium lead triiodide ($FAPbI_3$) was prepared by dissolving 4.13 g of the purified FAI and 11.06 g of PbI_2 in 30 mL of 2-methoxyethanol. The mixture was stirred vigorously at 120 °C for 1 h to yield black $FAPbI_3$ powder. The product was collected by filtration, washed with diethyl ether, and dried under vacuum at 60 °C for 24 h.

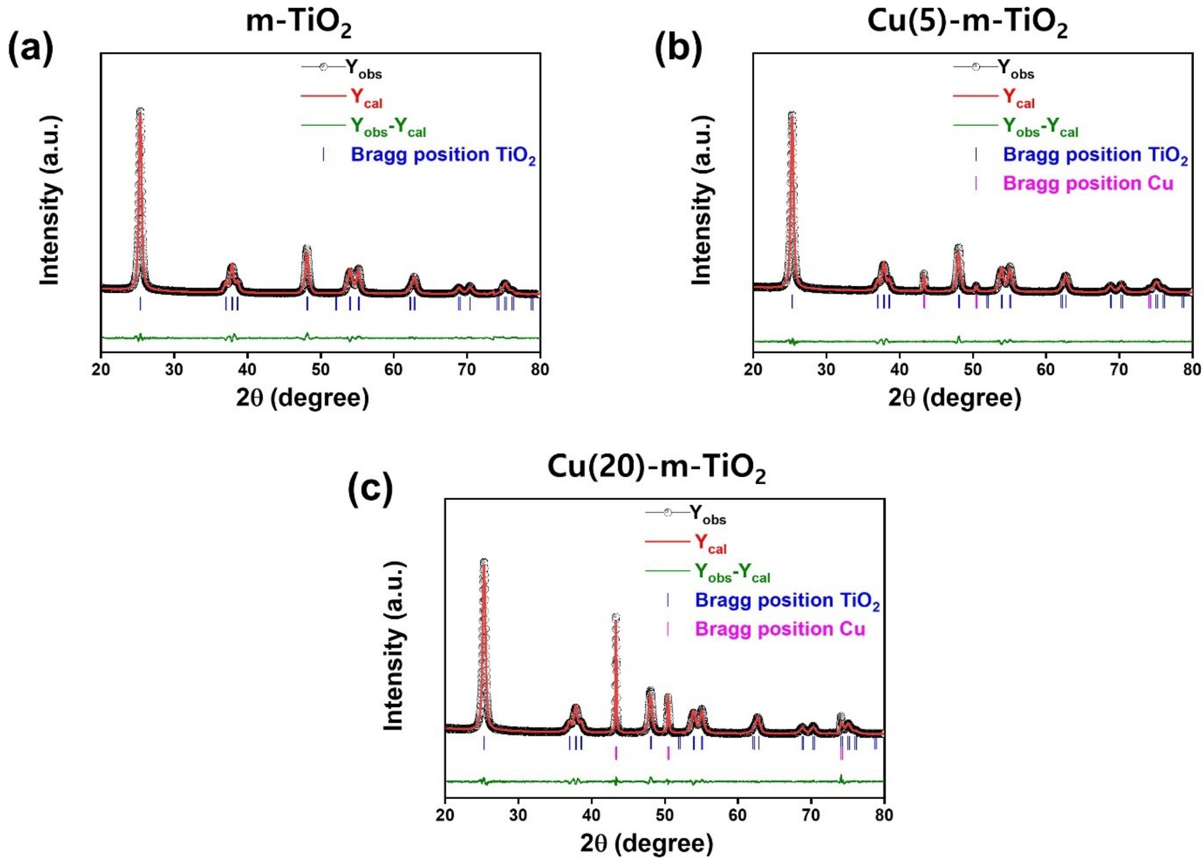

Figure S1. Rietveld calculated XRD patterns of (a) m-TiO_2, (b) Cu (5)-m-TiO_2, and Cu (20)-m-TiO_2 (20).

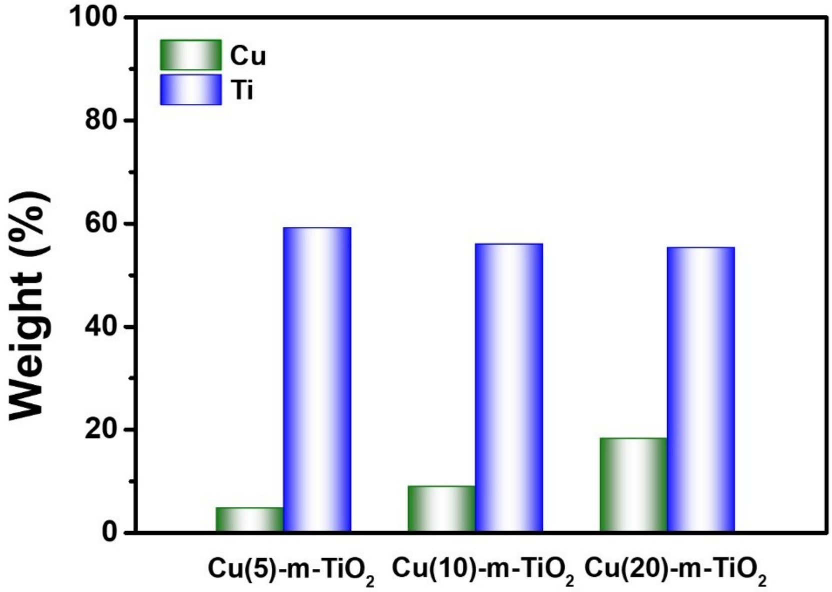

Figure S2. Weight percentage of Cu and Ti in Cu(5)-m-TiO_2, Cu(10)-m-TiO_2, and Cu(20)-m-TiO_2 determined by ICP-OES analysis.

Table S1. Weight percentage of Cu and Ti in Cu(5)-m-TiO_2, Cu(10)-m-TiO_2, and Cu(20)-m-TiO_2 as determined ICP-OES analysis.

Sample	Element	Weight (%)
5%	Cu	4.65
	Ti	59.06
10%	Cu	8.82
	Ti	55.88
20%	Cu	18.10
	Ti	55.15

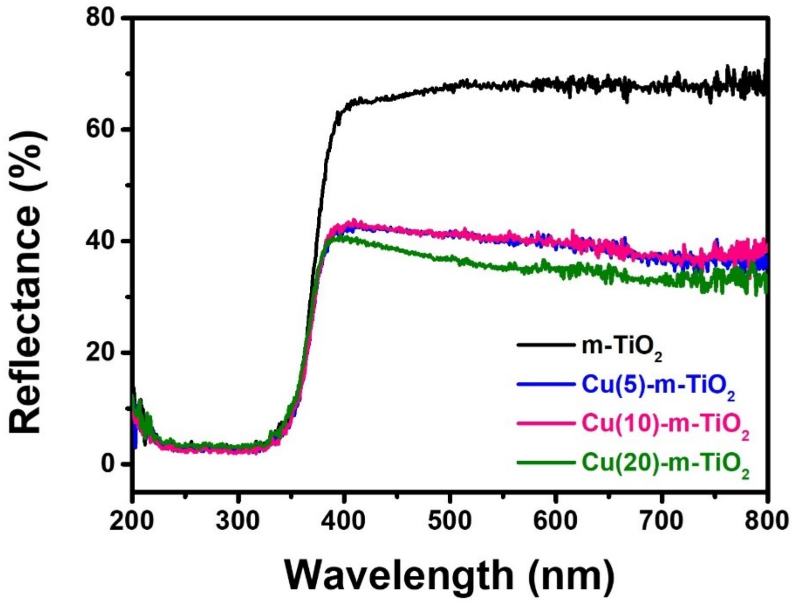

Figure S3. Reflectance spectra of the m-TiO_2, Cu(5)-m-TiO_2, Cu(10)-m-TiO_2, and Cu(20)-m-TiO_2.

Table S2. XPS Cu 2p peak positions, relative peak areas, and electronic states for Cu(5)-m-TiO_2, Cu(10)-m-TiO_2, and Cu(20)-m-TiO_2.

Sample	**Position (eV)**	**Relative peak Area (%)**	**Electronic state**
Cu(5)-m-TiO_2	932.38	48.86	Cu $2p_{3/2}$
	932.80	6.93	Cu_2O $2p_{3/2}$
	933.90	4.88	CuO $2p_{3/2}$
	947.49	9.02	Satellite
	952.27	23.56	Cu $2p_{1/2}$
	953.00	4.33	Cu_2O $2p_{1/2}$
	954.46	2.42	CuO $2p_{1/2}$
Cu(10)-m-TiO_2	932.77	50.14	Cu $2p_{3/2}$
	933.00	7.80	Cu_2O $2p_{3/2}$
	934.00	6.85	CuO $2p_{3/2}$
	947.83	5.34	Satellite
	952.51	22.18	Cu $2p_{1/2}$
	953.12	4.80	Cu_2O $2p_{1/2}$
	954.45	2.88	CuO $2p_{1/2}$
Cu(20)-m-TiO_2	932.36	50.19	Cu $2p_{3/2}$
	932.81	4.68	Cu_2O $2p_{3/2}$
	934.19	5.12	CuO $2p_{3/2}$
	945.34	4.83	Satellite
	952.24	29.76	Cu $2p_{1/2}$
	952.30	2.37	Cu_2O $2p_{1/2}$
	954.97	2.34	CuO $2p_{1/2}$

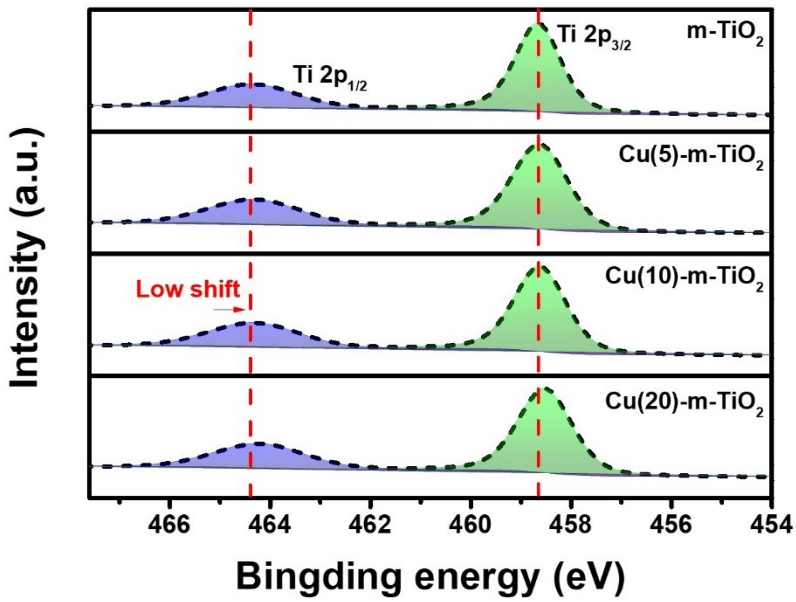

Figure S4. XPS spectra of Ti 2p for m-TiO_2, Cu(5)-m-TiO_2, Cu(10)-m-TiO_2, and Cu(20)-m-TiO_2.

Table S3. XPS Ti 2p peak positions, relative peak areas, and electronic states for Cu(5)-m-TiO_2, Cu(10)-m-TiO_2, and Cu(20)-m-TiO_2.

Sample	Position (eV)	Relative peak Area (%)	Electronic state
m-TiO_2	458.66	68.81	Ti $2p_{3/2}$
	464.34	31.19	Ti $2p_{1/2}$
Cu(5)-m-TiO_2	458.63	69.13	Ti $2p_{3/2}$
	464.31	30.87	Ti $2p_{1/2}$
Cu(10)-m-TiO_2	458.62	69.21	Ti $2p_{3/2}$
	464.31	30.79	Ti $2p_{1/2}$
Cu(20)-m-TiO_2	458.52	68.54	Ti $2p_{3/2}$
	464.20	31.46	Ti $2p_{1/2}$

Table S4. EIS parameters for m-TiO_2, Cu(5)-m-TiO_2, Cu(10)-m-TiO_2, and Cu(20)-m-TiO_2.

Sample	R_s(Ω)	R_{ct}(Ω)
m-TiO_2	3.28×10^1	1.52×10^5
Cu(5)-m-TiO_2	3.02×10^1	8.56×10^4
Cu(10)-m-TiO_2	3.08×10^1	7.82×10^4
Cu(20)-m-TiO_2	3.01×10^1	1.08×10^5

Table S5. Photovoltaic parameters of different Cu-m-TiO_2 ETL based PSCs.

ETLs		J_{SC} (mA/cm^2)	V_{OC} (V)	FF	PCE (%)
m-TiO_2	reverse	25.42	1.097	0.828	23.12
	forward	24.95	1.079	0.817	22.01
Cu(5)-m-TiO_2	reverse	25.83	1.12	0.82	24.01
	forward	25.46	1.11	0.79	22.49
Cu(10)-m-TiO_2	reverse	26.19	1.162	0.844	25.68
	forward	26.11	1.151	0.838	25.18
Cu(15)-m-TiO_2	reverse	26.24	1.13	0.82	24.52
	forward	25.81	1.12	0.81	23.50
Cu(20)-m-TiO_2	reverse	25.54	1.13	0.81	23.66
	forward	25.35	1.09	0.76	21.04

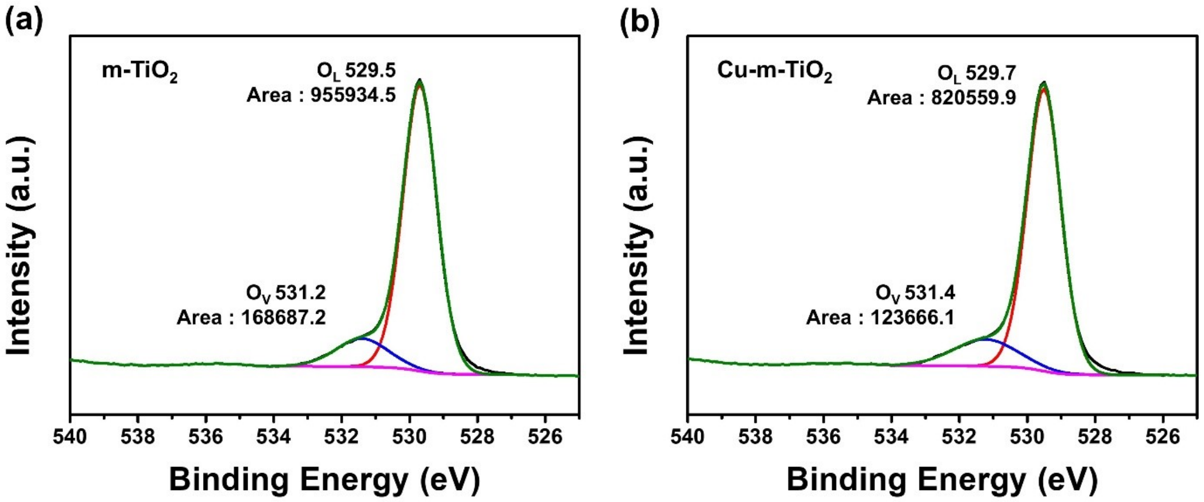

Figure S5. XPS spectra of O 1s for m-TiO_2 and Cu-m-TiO_2 layers after sintering.

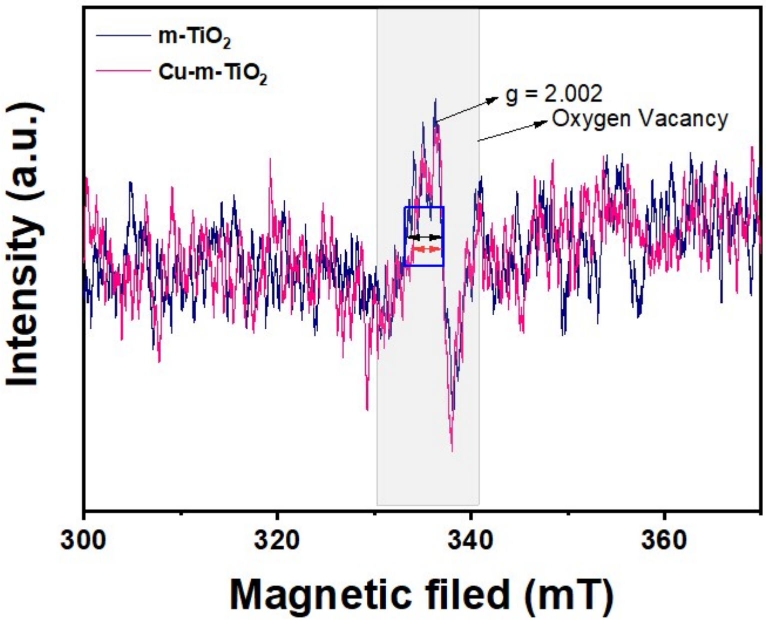

Figure S6. EPR spectra of m-TiO_2 and Cu-m-TiO_2.

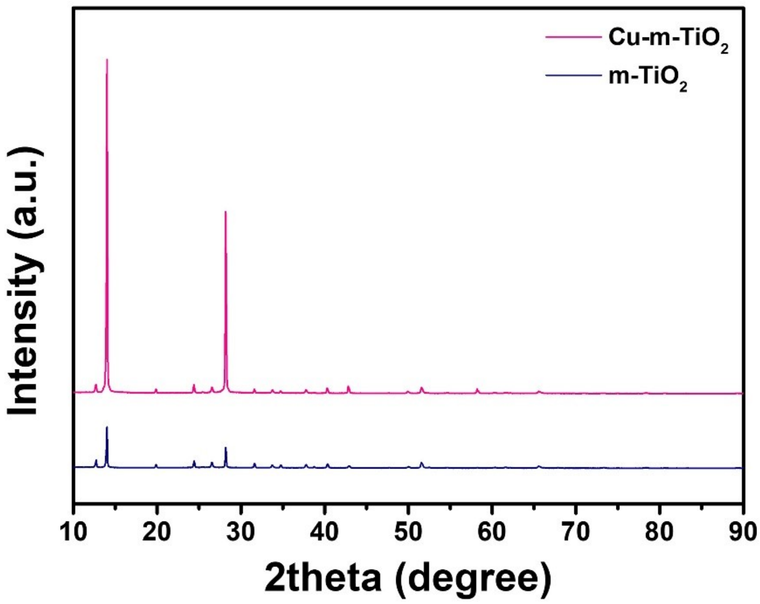

Figure S7. XRD patterns of $FAPbI_3$ films deposited on m-TiO_2 and Cu-m-TiO_2 electron transport layers.

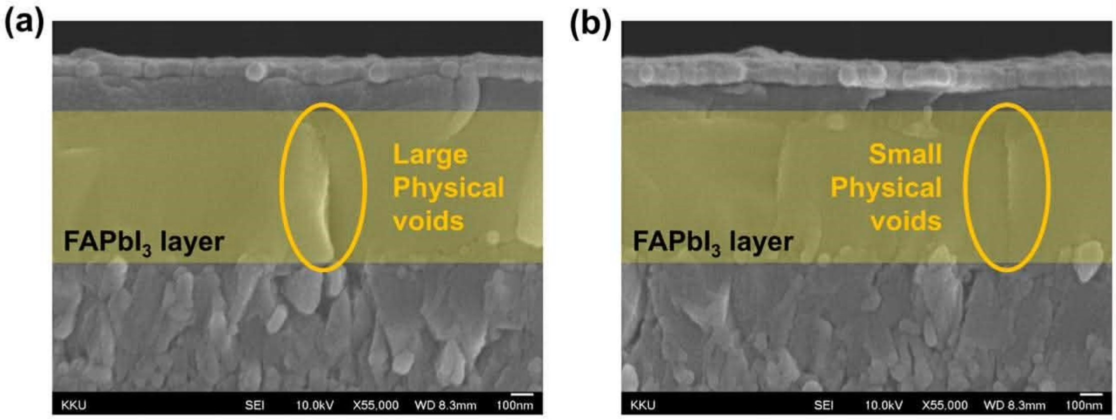

Figure S8. Cross-sectional FE-SEM images of complete devices employing (a) m-TiO_2 and (b) Cu-m-TiO_2, highlighting the grain boundaries and intergranular voids within the $FAPbI_3$ perovskite layer.

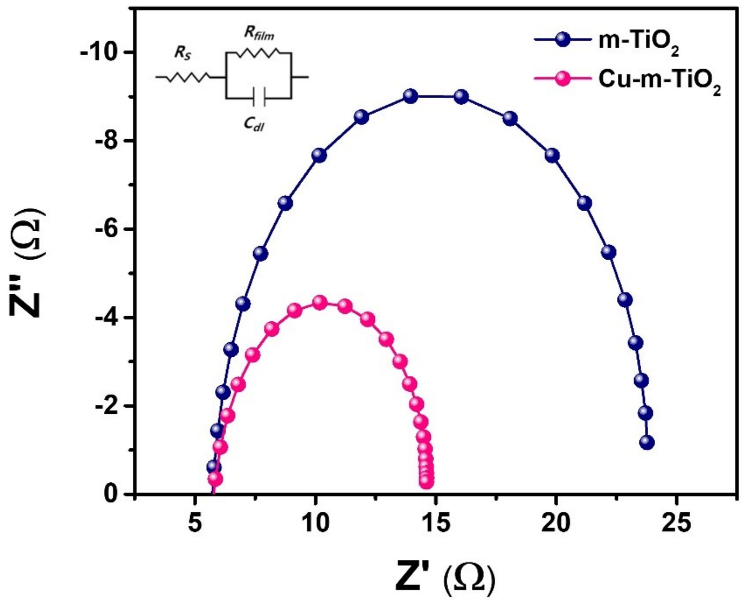

Figure S9. Nyquist plots of asymmetric devices with a configuration of FTO/m-TiO_2 (or Cu-m-TiO_2)/Au, measured in the frequency range from 1 MHz to 100 Hz under dark conditions, with an applied bias of 0.8 V and an AC amplitude of 10 mV. The inset shows the equivalent circuit used to fit the impedance spectra, where R_s represents the series (contact) resistance, R_{film} corresponds to the charge-transfer resistance of the m-TiO_2 (or Cu-m-TiO_2) film, and C_{dl} denotes the interfacial (double-layer) capacitance.

Effective electron conductivity and mobility calculation

The effective electrical conductivity (σ_{eff}) was determined from the film resistance (R_{film}) extracted from the Nyquist plots (Fig. S9) using the following relation:[S1]

$$\sigma_{eff} = \frac{l}{R_{eff}\,A}$$

where l is the thickness of the film (~175 nm), A is the electrode area (2 cm^2), and R_{film} is the film resistance obtained from EIS fitting. Accordingly, the calculated σ_{eff} values for m-TiO_2 and Cu-m-TiO_2 were 4.86×10^{-7} and 9.78×10^{-7} S/cm, respectively

The effective electron mobility (μ_{eff}) of m-TiO_2 and Cu-m-TiO_2 was calculated using the following equation:[S2]

$$\mu_{eff} = \frac{\sigma_{eff}}{q.n}$$

where q is the elementary charge of an electron, and n is the carrier concentration of m-TiO_2 and Cu-m-TiO_2, obtained from the Mott-Schottky analysis (Fig. 1e), which were 1.87×10^{21} and 2.65×10^{21} cm^{-3}, respectively. Based on these values, the calculated μ_{eff} values for m-TiO_2 and Cu-m-TiO_2 were 1.60×10^{-9} and 2.30×10^{-9} cm^2 V^{-1} s^{-1}, respectively.

Details of trap density (N_t) calculation

The trap-filled limit voltage (V_{TFL}) is identified at the intersection between the ohmic region and the trap-filled regime in the J-V curve. This characteristic voltage is then employed to evaluate the trap density (N_t) using the relation:[S3]

$$N_t = \frac{2 \in_0 \in_r V_{TFL}}{qL^2}$$

where ε_o is vacuum permittivity, ε_r is the relative dielectric constant of the $FAPbI_3$ (46.9),[S4] q is elementary charge (1.6×10^{-19} C), and L denotes the thickness of the perovskite layer (approximately 500 nm).

Details of biexponential function

$I = I_o + A_1 \exp\left(\frac{x}{\tau_1}\right) + A_2 \exp\left(\frac{x}{\tau_2}\right)$, corresponds to the fast decay component, primarily associated with interfacial charge transfer at the ETL/perovskite interface and τ_2 represents the slower decay process, arising from radiative recombination of free carriers within the bulk of the $FAPbI_3$ absorber. The average lifetime (τ_{avg}) was determined using the relation: $\tau_{avg} = (A_1\tau_1^2 + A_2\tau_2^2)/(A_1\tau_1 + A_2\tau_2)$.[S5]

Table S6. TRPL parameters of m-TiO_2 and Cu-m-TiO_2.

	A_1	τ_1 (ns)	A_2	τ_2 (ns)	$\tau_{avg.}$ (ns)
m-TiO_2	1509.5	1021.76	2020.8	227.06	839.54
Cu-m-TiO_2	1596.6	1004.27	2111.9	214.12	830.45

The photoluminescence decay transients obtained from TRPL were fitted with a bi-exponential function.[S5]

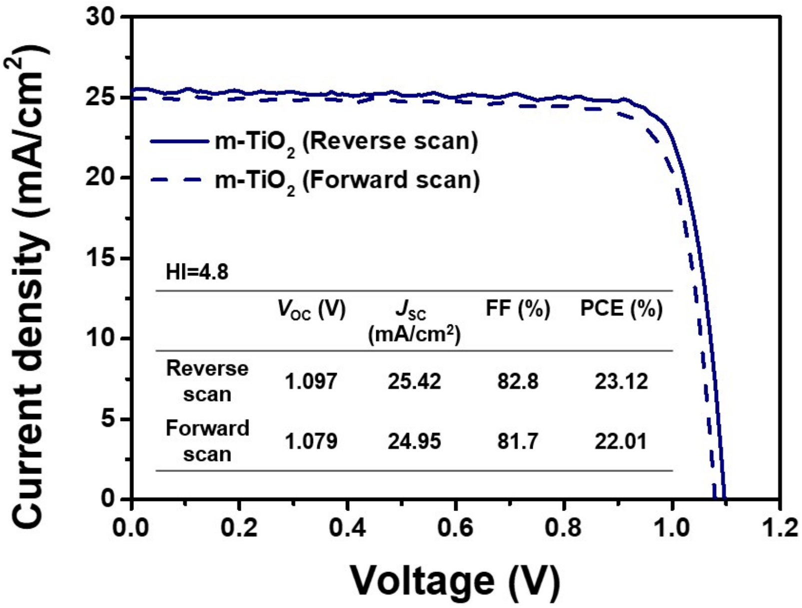

Figure S10. Forward and reverse scan *J–V* curves of PSCs employing m-TiO_2 (inset shows the summary of the corresponding PV parameters).

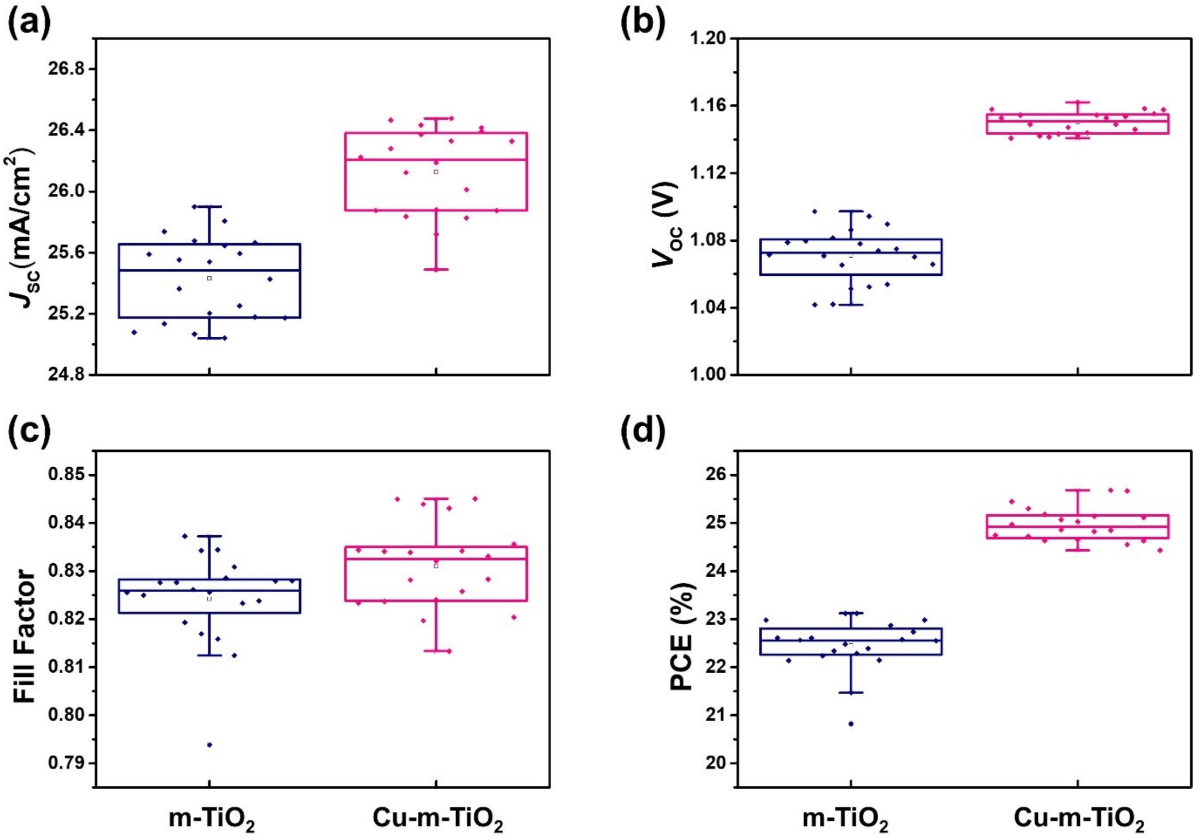

Figure S11. Statistical distribution of photovoltaic parameters: (a) J_{SC}, (b) V_{OC}, (c) FF, and (d) PCE for m-TiO_2 and Cu-m-TiO_2 based PSCs.

Table S7. Photovoltaic parameters PSCs with m-TiO_2.

Cell number	J_{SC} (mA/cm^2)	V_{OC} (V)	FF	PCE (%)
1	25.04	1.078	0.825	22.28
2	25.54	1.065	0.826	22.47
3	25.55	1.073	0.815	22.38
4	25.64	1.051	0.828	22.33
5	25.67	1.042	0.827	22.14
6	25.66	1.052	0.823	22.23
7	25.80	1.070	0.827	22.87
8	25.20	1.075	0.834	22.61
9	25.07	1.080	0.834	22.58
10	25.59	1.070	0.824	22.56
11	25.36	1.079	0.831	22.74
12	25.18	1.066	0.825	22.14
13	25.90	1.086	0.817	22.98
14	25.25	1.082	0.828	22.61
15	25.13	1.072	0.837	22.55
16	25.17	1.042	0.794	20.81
17	25.08	1.054	0.812	21.47
18	25.59	1.094	0.826	23.12
19 (Champion)	25.42	1.097	0.828	23.12
20	25.74	1.090	0.819	22.97
Average	25.43	1.071	0.824	22.45

Table S8. Photovoltaic parameters of PSCs with Cu-m-TiO_2.

Cell number	J_{SC} (mA/cm^2)	V_{OC} (V)	FF	PCE (%)
1	26.33	1.142	0.832	25.03
2	25.49	1.147	0.843	24.66
3	26.37	1.144	0.824	24.86
4	26.47	1.143	0.828	25.07
5	26.43	1.155	0.813	24.82
6	25.88	1.141	0.834	25.14
7	25.84	1.153	0.834	24.85
8	26.39	1.142	0.834	25.14
9	25.83	1.149	0.833	24.72
10	25.87	1.149	0.826	24.55
11	26.28	1.154	0.824	24.97
12	26.33	1.155	0.828	25.17
13 (Champion)	26.19	1.162	0.844	25.68
14	26.12	1.146	0.845	25.30
15	25.88	1.141	0.834	24.63
16	26.22	1.158	0.845	25.67
17	26.42	1.527	0.836	25.45
18	26.01	1.155	0.823	24.75
19	25.72	1.158	0.820	24.43
20	26.47	1.158	0.820	25.12
Average	26.15	1.151	0.830	24.99

References

[S1] K. A. Acord, A. D. Dupuy, Q. N. Chen, J. M. Schoenung, *J. Phys. Energy,* 2024, *6*, 025006.

[S2] V. Schmidt, P. F. J. Mensch, S. F. Karg, B. Gotsmann, P. D. Kanungo, H. Schmid, H. Riel, *Appl. Phys. Lett.,* 2014, *104*, 012113.

[S3] Q. Xiong, X. Huang, C. Wang, Q. Zhou, Y. Gang, T. Li, C. Hu, N. Zhang, X. Wang, J. Wu, Z. Su, X. Gao, X. Li, N. Zheng, P. Gao, *Joule,* 2024, *8*, 817–834.

[S4] F. Li, X. Huang, C. Ma, J. Xue, Y. Li, D. Kim, H.-S. Yang, Y. Zhang, B. R. Lee, J. Kim, B. Wu, S. H. Park, *Adv. Sci.,* 2023, *10*, 2301603.

[S5] M. M. Rahman, S. H. Won, H. D. Son, H. J. Jeong, T. W. Kim, *Mater. Today Energy,* 2025, *52*, 101939.